Variation in the distribution and properties of Circumpolar Deep Water in the eastern Amundsen Sea, on seasonal timescales, using seal-borne tags

Helen K. W. Mallett[1], Lars Boehme[2], Mike Fedak[2], Karen J. Heywood[1], David P. Stevens[1], and Fabien Roquet[3,4]

[1]Centre for Ocean and Atmospheric Sciences, University of East Anglia, Norwich, UK
[2]Sea Mammal Research Unit, University of St Andrews, UK
[3]Department of Meteorology, Stockholm University, Stockholm, Sweden
[4]Department of Marine Sciences, University of Gothenburg, Goteborg, Sweden

Key Points:

- In the eastern Amundsen Sea, the CDW layer is thicker in winter than in summer, and contains more heat and salt.
- On isopycnals, CDW is cooler and fresher in winter, likely the result of a rising core of offshelf CDW changing CDW properties onshelf.
- Farther south, in PIB, this seasonality is less pronounced, likely the result of mixing as the PIB gyre recirculates CDW of different ages.

Corresponding author: Karen J. Heywood, `k.heywood@uea.ac.uk`

Abstract

In the Amundsen Sea, warm saline Circumpolar Deep Water (CDW) crosses the continental shelf toward the vulnerable West Antarctic ice shelves, contributing to their basal melting. Due to lack of observations, little is known about the spatial and temporal variability of CDW, particularly seasonally. A new dataset of 6704 seal-tag temperature and salinity profiles in the easternmost trough between February and December 2014 reveals a CDW layer on average 49 db thicker in late winter (August to October) than in late summer (February to April), the reverse seasonality of that seen at moorings in the western trough. This layer contains more heat in winter, but on the 27.76 kg/m^3 density surface CDW is 0.32°C warmer in summer than winter, across the northeastern Amundsen sea, which may indicate wintertime shoaling off-shelf changes CDW properties onshelf. In Pine Island Bay these seasonal changes on density surfaces are reduced, likely by gyre circulation.

1 Introduction

Loss of the unstable West Antarctic ice sheet could produce sea level rise of 3.2 m [*Bamber et al.*, 2009] if it melts completely, of which approximately 40% by volume would drain via the Pine Island Glacier and Thwaites Glacier [*Payne et al.*, 2004]. The Pine Island Glacier is thinning [*Paolo et al.*, 2015] and accelerating [*Mouginot et al.*, 2014; *Rignot et al.*, 2014]. Warm, saline Circumpolar Deep Water (CDW) is implicated in this acceleration, flowing southward across the Amundsen Sea continental shelf from the open ocean and mixing with the shelf sea water masses. This modified CDW (henceforth CDW) is characterized by a subsurface temperature maximum, typically greater than 0°C, with absolute salinities greater than 34.7 g/kg. It flows beneath the thermocline at 350 to 650 m [*Jacobs et al.*, 2011; *Dutrieux et al.*, 2014], penetrating the Pine Island ice shelf cavity [*Jenkins et al.*, 1997], melting and thinning the ice shelf from below. This thinning reduces the buttressing provided by the ice shelf, allowing Pine Island Glacier to accelerate and thin [*Thomas*, 1979]. Identifying the spatial and temporal variability of CDW, and the mechanisms that drive this variability, is essential for validating the models that project the long term melt rates of Pine Island Glacier and the resultant sea level rise. Key questions include: how thick and how warm is the CDW layer near the continental shelf, how are the thickness and temperature of the CDW layer modified as it flows south to the Pine Island ice shelf cavity, and do the temperature and thickness vary seasonally.

CDW flows onto the Amundsen Sea continental shelf via three bathymetric troughs (Figure 1) [*Nitsche et al.*, 2007], the eastern and central of which lead to Pine Island ice shelf. For CDW to reach the ice shelf grounding line, it must overtop a ridge at 700 m depth within the cavity beneath the shelf [*Jenkins et al.*, 2010]. The temperature of the CDW between the cavity ceiling and the ridge (between 500 and 700 m) is particularly relevant for understanding basal melting of the ice shelf, as it provides the heat for this melting.

Oceanographic observations in the Amundsen Sea are limited. Ice-cover and harsh weather restrict ship access, limit mooring deployment and mooring retrieval, and prevent good spatial and temporal data coverage across the shelf. The vast majority of historical measurements in the Amundsen Sea are from summer, the only winter observations from a sparse distribution of moorings [*Heywood et al.*, 2016]. There are no near-surface winter observations, since drifting icebergs can catch and drag any mooring that is positioned too close to the surface. Thus, understanding of the seasonal variability on the shelf is severely restricted. Some models suggest a winter - spring (June - November) maximum in CDW onflow in the central trough as a result of seasonal changes in the wind field [*Thoma et al.*, 2008], with CDW thickness peaking in late winter - spring [*Thoma et al.*, 2008; *Steig et al.*, 2012]. *Schodlok et al.* [2012] modeled southward heat transport and CDW thickness peaking in fall (March-May) in the eastern trough, and *St-Laurent et al.* [2015] modeled a late winter (August-
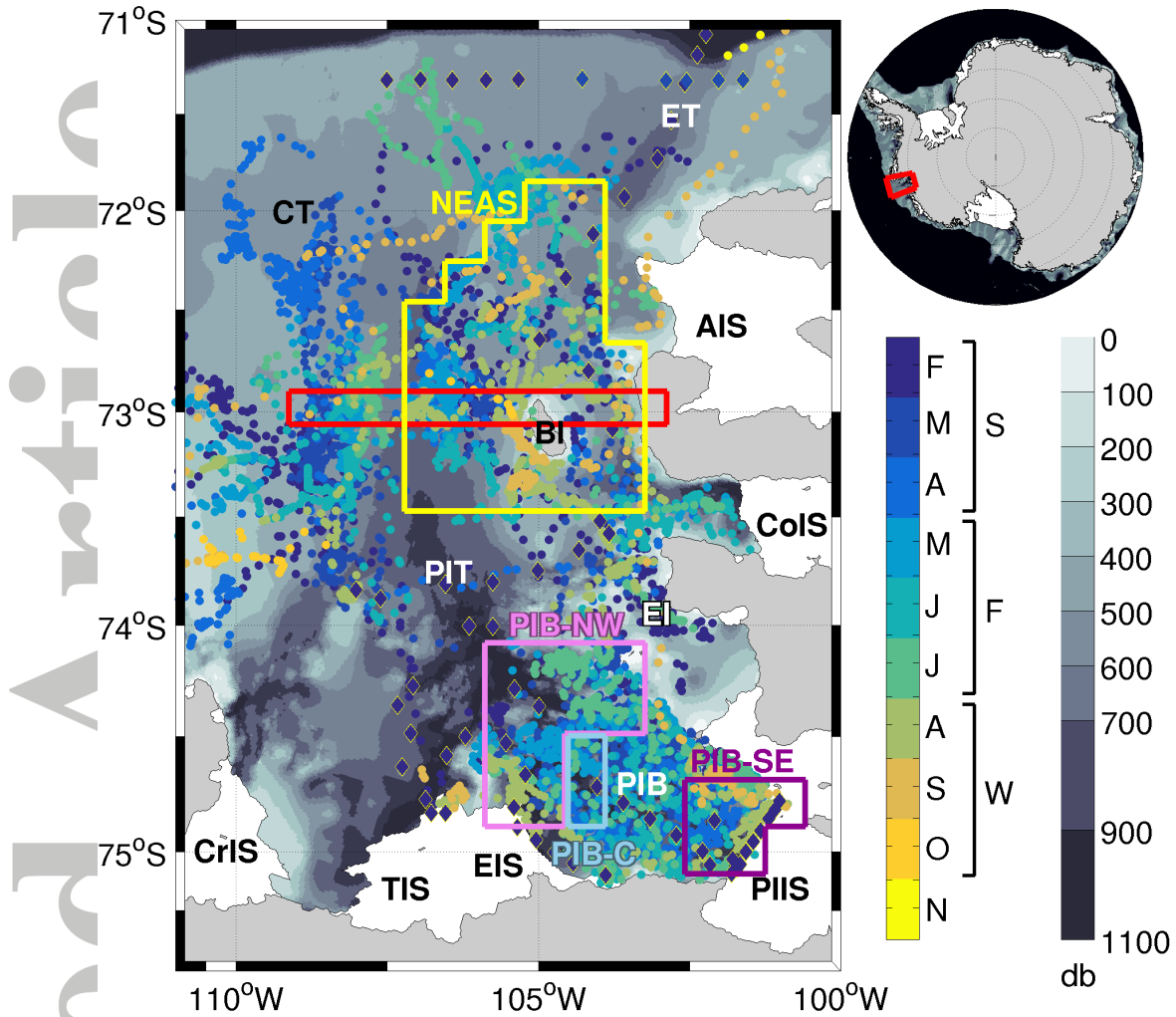
Figure 1. The eastern Amundsen Sea, with CTD profiles collected by seals (dots) and ship (diamonds), colored by date. Winter profile locations overlie some summer and fall locations. CTD locations overlie seal locations. The seasons used in analysis are marked alongside the date colorbar. Features marked: Crosson Ice Shelf (CrIS), Thwaites Ice Shelf (TIS), Eastern Ice Shelf (EIS), Pine Island Ice Shelf (PIIS), Cosgrove Ice Shelf (CoIS), Abbot Ice Shelf (AIS), Burke Island (BI), Eastern Trough (ET), Central Trough (CT), Pine Island Trough (PIT), Pine Island Bay (PIB) and the Edwards Islands (EI). The red rectangle contains the observations used for Figure 2. Marked in yellow, pink, blue and purple are the four regions used in Figure 4, north eastern Amundsen Sea (NEAS), Pine Island Bay north west (PIB-NW), Pine Island Bay central (PIB-C) and Pine Island Bay south east (PIB-SE). Inset is Antarctica, with the eastern Amundsen Sea marked in red. Bathymetry is IBCSO [*Arndt et al.*, 2013], coastline and grounding line are Bedmap2 in white and gray [*Fretwell et al.*, 2013].

October) minimum in heat content below 250 m at PIG. Nakayama et al. (2017) find no large seasonal variability at 552 m at the eastern trough shelf break, though they find January warmer and saltier than June at 222 m. . Year-round hydrographic observations are therefore needed to resolve this debate.

Previous work suggests that seasonal change in CDW thickness is different in different troughs. *Wåhlin et al.* [2013] found that both bottom temperature and CDW thickness peaked in fall (March-May) in the western trough, using mooring data collected between February 2010 and March 2012. In Pine Island Bay (PIB) a minimum in CDW thickness is seen in summer by *Webber et al.* [2017] using 5 years of mooring data, the reverse seasonality of that seen in the western trough. How representative the observations at these mooring locations are of the rest of their respective troughs remains to be assessed.

Here we investigate seasonal change in the location, properties and thickness of the CDW layer in the eastern trough using, to-date, the only dataset capable of providing the necessary broad spatial coverage through the seasons.

2 Methods

A total of 14 Conductivity-Temperature Depth - Satellite Relayed Data Loggers (CTD-SRDL, [*Boehme et al.*, 2009]) were deployed between 8th and 26th February 2014. 7 Southern Elephant seals (*Mirounga leonina*) were captured and tagged at the Edwards Islands (Figure 1, 73°52'S 102°59'W) and 7 Weddell seals (*Leptonychotes weddellii*) on sea ice between 72°23'S, 108°46'W and 72°56'S, 110°19'W. Half of the tags were still transmitting in September, with the last good quality measurements received on 1st December.

The tags reduce each conductivity-temperature-depth (CTD) profile into 17 or 18 depth levels using a broken-stick method, in order to maximize data transfer via the Argos satellite-based system [*Boehme et al.*, 2009; *Photopoulou et al.*, 2015]. This method samples the temperature maximum deeper than 100 db (ie CDW), and the temperature minimum. Only the deepest cast of every 4 hours is transmitted, ensuring the best possible temporal and spatial resolution for the limited battery power available and the data throughput limitations of the Argos system [*Boehme et al.*, 2009; *Fedak et al.*, 2002; *Fedak*, 2004].

Corrections were applied to the profile locations, derived using a Kalman smoother [*Lopez et al.*, 2015], and corrections to temperature and salinity were found from pre-deployment comparisons with ship-based CTD measurements. Profiles then underwent standard Delayed Mode Quality Control processing of the Marine Animals Exploring the Oceans Pole to Pole (MEOP) project ([*Roquet et al.*, 2011, 2013], http://www.meop.net/). The presented dataset has a nominal accuracy of +/-0.03° C for temperature and +/-0.05 for practical salinity [*Roquet et al.*, 2014] (absolute salinity accuracy can be considered comparable). It is estimated that the true accuracy of the salinity measurements is closer to +/-0.03, but as the conductivity sensor is known to introduce an extra offset when the CTD-SRDL is attached to the animal, we can use this accuracy estimate only as an indication. We use the TEOS-10 standard [*McDougall and Barker*, 2011]. There were 11,307 profiles successfully received by Argos, of which 10,838 passed quality control. 6,704 of these have both temperature and salinity measurements, are in the eastern Amundsen Sea and are used in the following analysis.

In the following analysis we group the profiles into regions to enable comparison between the seasons, and grid into cells 23 km latitudinally by 22 km longitudinally. We focus on the eastern shelf, where the warmest CDW was observed, and particularly near Burke Island and in PIB, where there are sufficient numbers of profiles throughout the observation period to make statistically robust seasonal comparisons (Figure 1). We also extract sections from the dataset, using an elongated rectangular area to approximate a linear section with a meridional range of 18 km (Figure 1).

We include 105 ship-based CTD profiles (diamonds, Figure 1), collected between 1st February and 5th March 2014 as part of the iSTAR JR294/295 cruise [*Heywood et al.*, 2016]. Seasonal analysis would not be possible with the ship-CTD measurements alone, as they are all from summer. These ship-based CTD profiles have a much higher vertical resolution. Both seal and ship-based observations are vertically gridded onto

a pressure grid of resolution 1 db and a density grid of resolution 0.00167 kg/m^3. Subsequent analysis does not differentiate between data sources. By number of profiles, the seal tag profiles provide 98.8% of the final dataset.
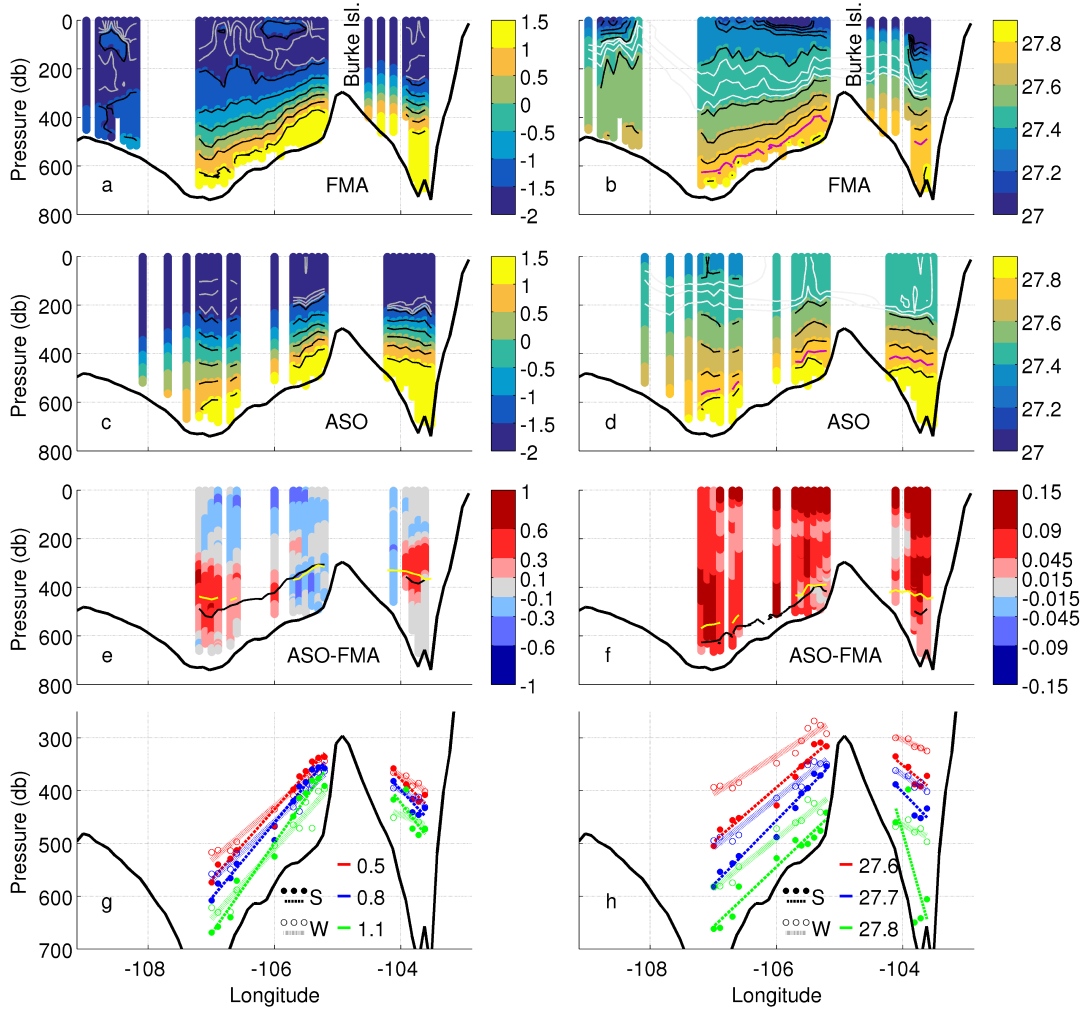
Figure 2. Conservative temperature of the section marked (Figure 1, red rectangle) for summer (a) and winter (c), averaged into 0.1° longitude bands. Black contours are 1.5 to -1.5°C isotherms in increments of 0.5°C. Gray contours are -1.5, -1.6, -1.7 and -1.8°C isotherms. The thick black line is the deepest bathymetry within each 0.1° longitude band of the section (IBCSO, [*Arndt et al.*, 2013]). (e) difference in temperature, winter - summer, where observations are available in both seasons. Red means water is warmer in winter than summer. Black and yellow lines are 0°C isotherms in summer and winter respectively. (g) the slope of the 0.5, 0.8 and 1°C isotherms in summer and winter. Dots are the seal observations, lines are linear regression, one each side of Burke Island. (b,d) as in (a,c) but for potential density anomaly. Black contours are 27 to 27.9 isopycnals in increments of 0.1, and white contours are the 27.425, 27.450, and 27.475 isopycnals. The purple contour is the 27.76 isopycnal. (f) as in (e) but for potential density anomaly. Black and yellow lines are 27.76 isopycnals in summer and winter respectively. (h) as in (g) but for the 27.6, 27.7 and 27.8 isopycnals

In order to separate observations of seasonality that result from changes in flow, from those that result from changes to the CDW properties, we examine seasonal differences on isopycnal surfaces. For this we choose the 27.76 kg/m^3 isopycnal (unit for density omitted hereafter), a surface approximately 100 db shallower than the core of the CDW, shallow enough for many seal profiles to sample it, but close enough to the core to behave similarly (Figure 2b and 2d). The 0°C isotherm can be considered the upper boundary of the CDW layer.

For four regions of interest (Figure 1) we calculate median profiles of conservative temperature against potential density anomaly, averaged on density, where at least 10 profiles are available, and using only observations in cells where data are available in all relevant seasons. Profiles are first averaged into cells, and then between the cells within a region, to eliminate regional bias. Only profiles that are sufficiently deep to reach water warmer than 0°C are included. Median profiles are also calculated for potential density anomaly, conservative temperature and absolute salinity against pressure, averaged on pressure.

These regions of interest are chosen where properties and seasonality are broadly consistent. The northeastern Amundsen Sea region (Figure 1) covers a large area where observations from all seasons are present and oceanographic conditions are similar. PIB is separated into three regions with different seasonal changes in the depth of the 27.76 isopycnal. There are insufficient observations in the rest of the Amundsen Sea for robust seasonal analysis.

Using cells near Burke Island and profiles offshelf at the eastern trough (Figure 3g), we compare the properties of source CDW with those onshelf by calculating mean conservative temperature and absolute salinity profiles for different seasons, averaged on density, to determine if changes in the depth of the isopycnals offshelf are responsible for some of the observed seasonal changes in CDW properties.

For this seasonal analysis we compare late summer (February, March and April (FMA), henceforth 'summer'), with late fall (May, June and July (MJJ), henceforth 'fall'), and with late winter (August, September and October (ASO), henceforth 'winter'). Since there are few seal observations from November to January, these three seasons best represent the extrema of winter and summer from the available data. The addition of one or two fall months to the end of summer or to the beginning of winter, when comparing summer and winter, makes little difference to the conclusions drawn. There are many more observations in summer than winter, since more tags fail as the year progresses, so we compare the seasons only in locations where observations from both seasons are available.

3 Results

A zonal section north of Burke Island (Figure 1) reveals that the upper 150 m experiences the expected seasonal cycle of ice-melt freshening in summer, and surface cooling, mixed layer deepening and surface salinification from sea ice formation in winter (Figure 2, and for salinity, Figure S1). The effect of salinification is detectable from the associated potential density anomaly (Figures 2b, 2d and 2f). Below 300 db, isotherms are shallower in winter than in summer, the CDW layer is warmer in winter than in summer on pressure surfaces (Figure 2e), and more saline (Figure S1. An exception, just west of Burke Island where the deep isotherms, isohalines and isopycnals are locally deeper in winter than in summer (blue, Figures 2e and 2f), could be due to a small scale (approximately 10 km) westward shift in the isopycnals, resulting from a winter westward shift or decrease in the speed of the southward current here. Throughout the section, isopycnals (and isohalines) are shallower in winter, thus a thicker CDW layer is present, and this CDW layer is denser in winter than in summer on pressure surfaces. Between 107°W and 105.2°W, west of Burke Island, the deep isopycnals and isotherms are steeper in summer, suggesting faster flow (Figures 2g and 2h).
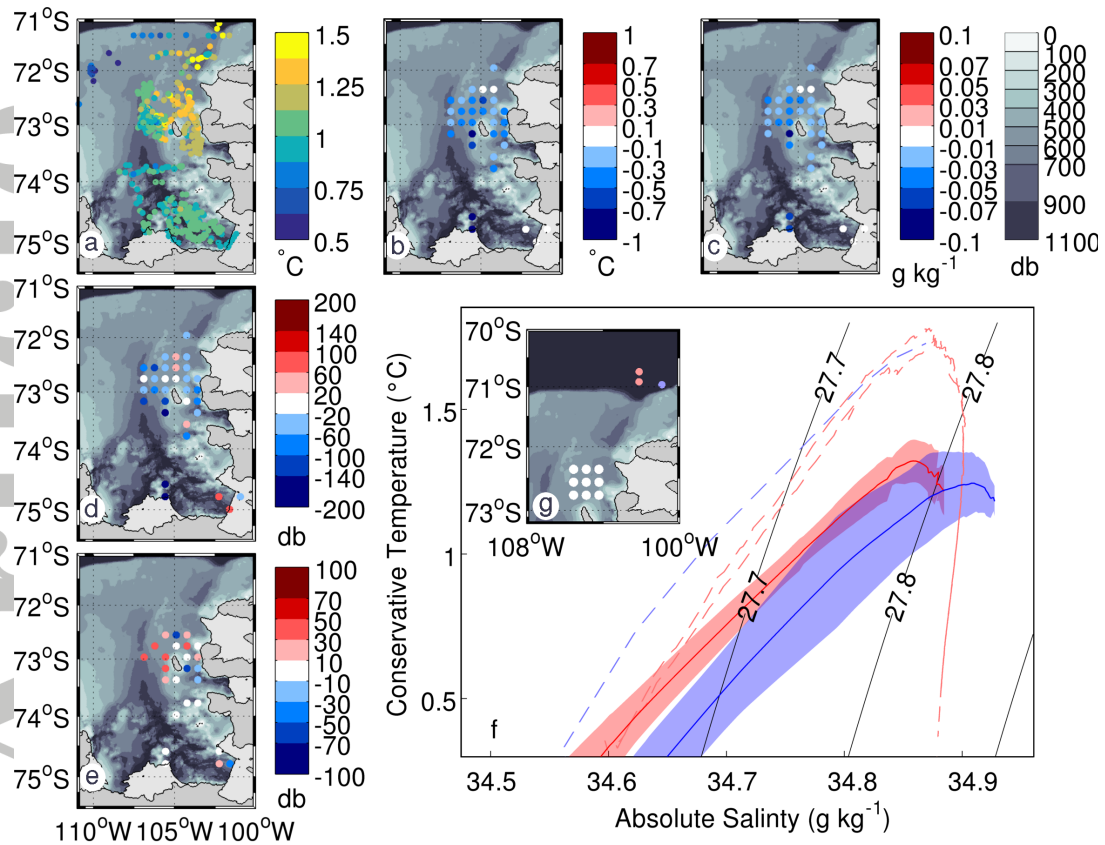
Figure 3. Conservative temperature on the 27.76 isopycnal in summer (a). (b) difference in conservative temperature, winter minus summer, on the 27.76 isopycnal, where red means winter is warmer than summer. Observations are gridded in longitude and latitude on isopycnal surfaces, enabling comparison between seasons. (c) as (b), but for absolute salinity in g/kg. (d) as (b), but showing difference in pressure of 27.76 isopycnal, where red means the isopycnal is deeper in winter. (e) difference in thickness of the CDW layer beneath the 0°C isotherm, winter minus summer, where red means the CDW layer in winter is thicker than summer. (f) conservative temperature and absolute salinity of a group of cells onshelf in winter (blue) and summer (red), shading indicating standard deviation. Dashed lines are profiles offshelf near the eastern trough in winter (blue) and summer (red). Black lines are isopycnals. (g) locations of these cells (white) and offshelf profiles (pale red and pale blue).

In the northeastern Amundsen Sea, between 71°S and 74°S and east of 111°W, the CDW layer underneath the 0°C isotherm is on average 5.6 db thicker in winter than in summer. This is variable over distances as small as 20 km, though coherent thickness change is observed over distances up to 100 km (Figure 3e). The mean temperature of this CDW layer, where both winter and summer data are available, is not measurably different.

On the 27.76 isopycnal the warmest water on the continental shelf was in the eastern trough in February, at 1.64°C (Figure 3a). The CDW flows south both via Pine Island Trough and east of Burke Island (Figure 3a). It is not possible to judge whether or how much CDW arrives at PIB via the central trough, since the observations are sparse at the confluence of the two troughs. The warmest CDW in PIB, on the same isopycnal, is in May at 1.09°C, a reduction of 0.55°C from the shelf break temperature.

The 27.76 isopycnal is shallower in winter than summer through much of the northeastern Amundsen Sea (Figure 3d), by an average of 49 db, thus the CDW layer is thicker in winter. The 27.76 isopycnal, deeper than the 0°C isotherm, deepens farther south. The depth of the 0°C isotherm is also greater farther south, but to a much lesser degree, and is more variable on spatial scales of the order 20 km. As such the 27.76 isopycnal is considered a more reliable judge of CDW layer thickness change than the 0°C isotherm. The 27.76 isopycnal is warmest and most saline in summer and coolest and freshest in winter (Figures 3b and 3c). Summer is an average of 0.32 °C warmer than winter, using an area-weighted average where observations for both seasons are available (Figure 3b). Adjustments to the choice of isopycnal surface do not change the conclusions.

In the northeastern Amundsen Sea, isopycnals deeper than 200 db are shallower in winter than summer by approximately 100 db (Figure 4i). The pressures of isopycnals between 100 and 500 db are very similar in fall to those in summer. Below 500 db, in the CDW water mass, the pressures of isopycnals in fall are between those in summer and winter, suggesting that here the CDW layer thickness increases gradually from summer to winter. Temperatures are between 0.2 and 0.5°C colder in winter than in summer on isopycnals in the northeastern Amundsen Sea (Figure 4e). For cells north of Burke Island (Figure 3g), the mean winter profile in temperature - salinity space has a cooler and deeper endpoint from within the offshelf source CDW water than the mean summer profile (Figure 3f).

In PIB North West (PIB-NW, pink, Figure 1) isopycnals deeper than 500 db are approximately 200 db shallower and up to 0.3°C cooler in fall than summer (Figures 4j and 4f). In PIB Central (PIB-C, blue, Figure 1), adjacent to PIB-NW, isopycnals deeper than 500 db are up to 200 db deeper in fall than in summer (Figure 4k), the reverse of the seasonality seen in PIB-NW at the same depths. In PIB South East (PIB-SE, purple, Figure 1), the mixed layer deepens from near-surface in summer to approximately 350 db in winter. Below 500 db, seasonal differences in temperature, salinity and density are minimal.

4 Discussion

Across much of the northeastern Amundsen Sea, we find a thicker CDW layer in winter, which contains more heat and more salt, but which is cooler and fresher in winter on the 27.76 isopycnal. Seasonal changes across PIB are not coherent, and are highly variable at spatial scales as small as 20km. A divergence in the depth of the 0°C isotherm and the deeper 27.76 isopycnal as CDW flows south (not shown) suggests that more mixing takes place as CDW flows south, such that CDW in PIB no longer displays the same clear seasonal differences that are observed in the northeastern Amundsen Sea. It is likely that the rotating PIB gyre contributes greatly to this mixing, recirculating and combining CDW that entered the continental shelf at different times.

Thoma et al. [2008] and *Steig et al.* [2012] modeled a CDW layer approximately 20 m thicker in winter than summer, between 1980 and 1999 using a coupled ocean - sea ice model with daily mean forcing from the NCEP/NCAR reanalysis. The observed seasonal cycle in CDW layer thickness (thicker in winter) is the reverse of that previously observed in the western trough [*Ha et al.*, 2014; *Kim et al.*, 2017; *Wåhlin et al.*, 2013]. This opposite seasonality could be a result of seasonal shift in the main route of CDW inflow between the troughs, raising CDW thickness in the western trough in summer and the eastern trough in winter. Simultaneous mooring arrays spanning all troughs would be necessary to investigate this.

Using an optimized simulation *Nakayama et al.* [2017] find no large seasonal variability in CDW properties at 552 m at the eastern trough shelf break. Although there are insufficient seal tag profiles for seasonal comparison at the shelf break, nearby profiles in the northeastern Amundsen Sea show pronounced seasonal differences (Figure
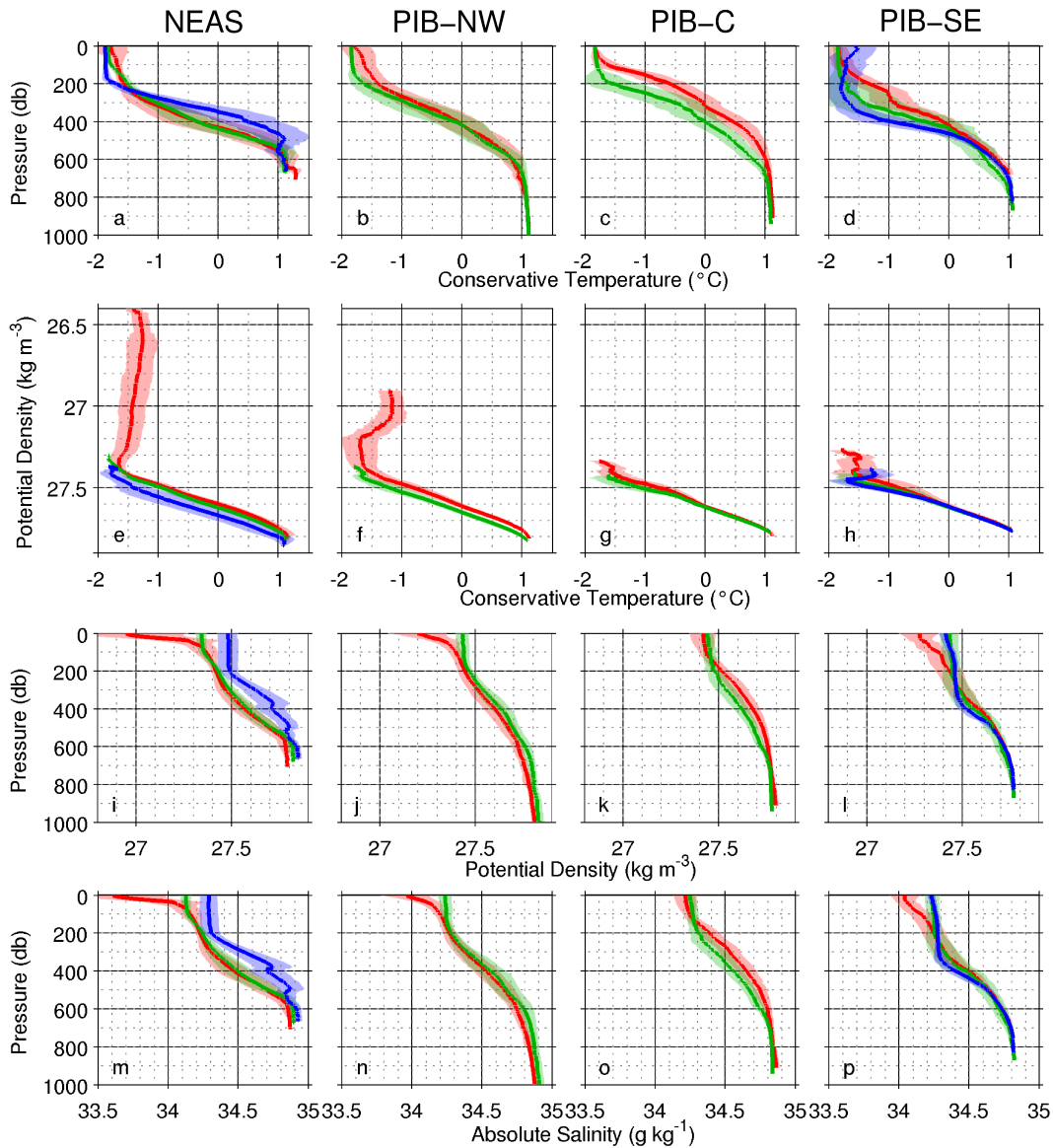
Figure 4. Median profiles and standard deviations (pastel shading) for summer (red), fall (green) and winter (blue) for regions marked in Figure 3e. Means are very similar to the medians and so are omitted. (a) profiles of conservative temperature against pressure. Profiles are from the northeastern Amundsen Sea, including only cells where data for both summer and winter are available. (e) profiles of conservative temperature against potential density anomaly, for the same region. (i) profiles of potential density against pressure. (m) profiles of absolute salinity against pressure. (b,f,j,n) as in (a,e,i,m), but for PIB-NW, for only cells where profiles from both summer and fall are available. There are less than 10 profiles in winter, so the winter average profiles are not plotted. (c,g,k,o) as in (b,f,j,n), but for PIB-C. (d,h,l,p) as in (a,e,i,m), but for PIB-SE.

3f), unlike the model. The model of *St-Laurent et al.* [2015] produced a late winter (August-October) minimum in heat content below 250 m at PIG, which agrees with our observations, although we observe minimum seasonality in the deep core CDW (Figure 4d).

The cooler, saltier CDW endpoint in winter in the northeastern Amundsen Sea (Figure 3f) is likely the result of a shoaling of winter isopycnals offshelf, such that a denser, cooler and saltier CDW is able to flow onto the continental shelf. This offshelf shoaling would also produce a thicker CDW layer. A denser CDW source water can be of the order of 0.5°C cooler [*Wåhlin et al.*, 2013]. If this were to mix with surface waters it might reach the same density as CDW from a less dense, warmer source. Winds can raise the thermocline at the shelf break through Ekman pumping [*Dutrieux et al.*, 2014]. Though there are no concurrent moorings offshelf at the eastern trough to corroborate this winter shoaling, an onshelf mooring (unpublished) near to the shelf break does observe a raised thermocline between May and October 2014.

Webber et al. [2017] find an interannual variability of temperature of the order of 1°C at 500 db and 0.3°C at 700 db in the area close to PIB. In comparison to this, our seasonal change of 0.32°C in CDW temperatures on the 27.76 isopycnal (at approximately 600 db) over the northeastern Amundsen sea is considerable, although few comparisons are available in PIB. This suggests that the summer-biased historical dataset may misrepresent interannual change and variability of CDW in the Amundsen Sea. Previously, seasonal changes seen at single moorings might have been due to current cores shifting location seasonally across the moorings. Here we demonstrate that coherent changes occur over areas on the scale of approximately 150 km.

The water mass changes observed by the seal tags are inevitably a superposition of seasonal and interannual changes [*Webber et al.*, 2017]. With only one year of seal tag data it is not possible to separate these. However the seasonality that we document is consistent with that observed at the moorings in Pine Island Bay [*Webber et al.*, 2017] and with the seasonal cycle in CDW layer thickness in the model results of *Steig et al.* [2012].

A cyclonic gyre in PIB [*Thurnherr et al.*, 2014] is observed in the seal data by *Heywood et al.* [2016]. The opposite seasonal changes in CDW thickness between the neighboring PIB-C and PIB-NW regions could be explained by a slowing of this gyre in fall. Such a slowing would reduce the doming of the isopycnals and produce the observed pattern, if PIB-C were at the center of the gyre, and PIB-NW were at the edge of the gyre. An alternative explanation is a lateral movement in the location of the gyre between summer and fall, raising isopynals on one side of the gyre and depressing them on the other. Changes associated with this gyre are likely to be largely responsible for the reduced seasonal differences observed on density surfaces nearer Pine Island Glacier, compared with the northeastern Amundsen Sea, as the gyre recirculates and mixes together CDW that entered onto the continental shelf at different times.

5 Conclusions

The warmest CDW of the Amundsen Sea is found in the eastern trough. Throughout most of the eastern Amundsen Sea there is a thicker layer of CDW in winter than in summer, which contains more heat and salt in winter, but which is cooler and fresher in winter on isopycnals. This is particularly prominent in the northeastern Amundsen Sea. This combination of seasonal differences could be the result of shoaling of isopycals offshelf at the eastern trough, allowing a thicker layer of CDW onto the continental shelf, and allowing denser, cooler and saltier CDW access to the shelf, changing the endpoint of the onshelf CDW between winter and summer. This seasonality is much reduced in PIB, likely the result of the recirculating water in the PIB gyre. The observed seasonality in CDW thickness in the northeastern Amundsen Sea is reversed from that seen previously in the western trough [*Wåhlin et al.*, 2013].

The observations presented here enable the first comprehensive analysis of seasonal change in CDW across the eastern Amundsen Sea. This study provides a foundation for future research to separate seasonal variability from interannual variability in this crucial region for understanding and predicting future sea level rise.

Acknowledgments

References

Arndt, J. E., Schenke, H. W., Jakobsson, M., Nitsche, F. O., Buys, G., Goleby, B., Rebesco, M., Bohoyo, F., Hong, J., Black, J., Greku, R., Udintsev, G., Barrios, F., Reynoso-Peralta, W., Taisei, M., and Wigley, R. (2013). The International Bathymetric Chart of the Southern Ocean (IBCSO) Version 1.0-A new bathymetric compilation covering circum-Antarctic waters. *Geophysical Research Letters*, 40(12):3111–3117.

Bamber, J. L., Riva, R. E. M., Vermeersen, B. L. A., and LeBrocq, A. M. (2009). Reassessment of the Potential Sea-Level Rise from a Collapse of the West Antarctic Ice Sheet. *Science*, 324:901–903.

Boehme, L., Lovell, P., Biuw, M., Roquet, F., Nicholson, J., Thorpe, S. E., Meredith, M. P., and Fedak, M. (2009). Technical Note: Animal-borne CTD-Satellite Relay Data Loggers for real-time oceanographic data collection. *Ocean Sci*, 5:685–695.

Dutrieux, P., De Rydt, J., Jenkins, A., Holland, P. R., Ha, H. K., Lee, S. H., Steig, E. J., Ding, Q., Abrahamsen, E. P., and Schroder, M. (2014). Strong Sensitivity of Pine Island Ice-Shelf Melting to Climatic Variability. *Science*, 343(6167):174–178.

Fedak, M., Lovell, P., McConnell, B., and Hunter, C. (2002). Overcoming the Constraints of Long Range Radio Telemetry from Animals: Getting More Useful Data from Smaller Packages. *Integrative and Comparative Biology*, 42:3–10.

Fedak, M. (2004). Marine animals as platforms for oceanographic sampling: a win/win situation for biology and operational oceanography. *Memoirs of National Institute of Polar Research Special Issue*, 58:133–147.

Fretwell, P., Pritchard, H. D., Vaughan, D. G., Bamber, J. L., Barrand, N. E., Bell, R., Bianchi, C., Bingham, R. G., Blankenship, D. D., Casassa, G., Catania, G., Callens, D., Conway, H., Cook, A. J., Corr, H. F. J., Damaske, D., Damm, V., Ferraccioli, F., Forsberg, R., Fujita, S., Gim, Y., Gogineni, P., Griggs, J. A., Hindmarsh, R. C. A., Holmlund, P., Holt, J. W., Jacobel, R. W., Jenkins, A., Jokat, W., Jordan, T., King, E. C., Kohler, J., Krabill, W., Riger-Kusk, M., Langley, K. A., Leitchenkov, G., Leuschen, C., Luyendyk, B. P., Matsuoka, K., Mouginot, J., Nitsche, F. O., Nogi, Y., Nost, O. A., Popov, S. V., Rignot, E., Rippin, D. M., Rivera, A., Roberts, J., Ross, N., Siegert, M. J., Smith, A. M., Steinhage, D., Studinger, M., Sun, B., Tinto, B. K., Welch, B. C., Wilson, D., Young, D. A., Xiangbin, C., and Zirizzotti, A. (2013). Bedmap2: improved ice bed, surface and thickness datasets for Antarctica. *The Cryosphere*, 7(1):375–393.

Ha, H. K., Wåhlin, A. K., Kim, T. W., Lee, S. H., Lee, J. H., Lee, H. J., Hong, C. S., Arneborg, L., Björk, G., and Kalén, O. (2014). Circulation and Modification of Warm Deep Water on the Central Amundsen Shelf. *Journal of Physical Oceanography*, 44(5):1493–1501.

Heywood, K., Biddle, L., Boehme, L., Dutrieux, P., Fedak, M., Jenkins, A., Jones, R., Kaiser, J., Mallett, H., Naveira Garabato, A., Renfrew, I., Stevens, D., and Webber, B. (2016). Between the Devil and the Deep Blue Sea: The Role of the Amundsen Sea Continental Shelf in Exchanges Between Ocean and Ice Shelves. *Oceanography*, 29(4):118–129.

Jacobs, S. S., Jenkins, A., Giulivi, C. F., and Dutrieux, P. (2011). Stronger ocean circulation and increased melting under Pine Island Glacier ice shelf. *Nature Geoscience*, 4(8):519–523.

Jenkins, A., Vaughan, D. G., Jacobs, S. S., Hellmer, H. H., and Keys, J. R. (1997). Glaciological and oceanographic evidence of high melt rates beneath Pine Island Glacier, West Antarctica. *Journal of Glaciology*, 43(143):114–121.

Jenkins, A., Dutrieux, P., Jacobs, S. S., McPhail, S. D., Perrett, J. R., Webb, A. T., and White, D. (2010). Observations beneath Pine Island Glacier in West Antarctica and implications for its retreat. *Nature Geoscience*, 3(7):468–472.

Kim, T., Ha, H., Wåhlin, A., Lee, S., Kim, C., Lee, J., and Cho, Y. (2017). Is Ekman pumping responsible for the seasonal variation of warm circumpolar deep water in the Amundsen Sea? *Continental Shelf Research*, 132:38–48.

Lopez, R., Malardé, J. P., Danès, P., and Gaspar, P. (2015). Improving Argos Doppler location using multiple model smoothing. *Animal Biotelemetry*, 52(8):1–9.

McDougall, T. J. and Barker, P.M. (2011). Getting started with TEOS-10 and the Gibbs Seawater (GSW) Oceanographic Toolbox. *SCOR/IAPSO WG127*, 28pp., ISBN 978-0-646-55621-5.

Mouginot, J., Rignot, E., and Scheuchl, B. (2014). Sustained increase in ice discharge from the Amundsen Sea Embayment, West Antarctica, from 1973 to 2013. *Geophysical Research Letters*, 41(5):1576–1584.

Nakayama, Y., Menemenlis, D., Schodlok, M., and Rignot, E. (2017). Amundsen and Bellinghausen Seas simulation with optimized ocean, sea ice, and thermodynamic ice shelf model parameters. *Journal of Geophysical Research: Oceans*, 122:6180-6195.

Nitsche, F. O., Jacobs, S. S.., Larter, R. D., and Gohl, K. (2007). Bathymetry of the Amundsen Sea continental shelf: Implications for geology, oceanography, and glaciology. *Geochemistry Geophysics Geosystems*, 8(10):1–10.

Paolo, F. S., Fricker, H. A., and Padman, L. (2015). Volume loss from Antarctic ice shelves is accelerating. *Science*, 348(6232):327–331.

Payne, A. J., Vieli, A., Shepherd, A. P., Wingham, D. J., and Rignot, E. (2004). Recent dramatic thinning of largest West Antarctic ice stream triggered by oceans. *Geophysical Research Letters*, 31(23):1–4.

Photopoulou, T., Fedak, M. A., Matthiopoulos, J., McConnell, B., and Lovell, P. (2015). The generalized data management and collection protocol for Conductivity-Temperature-Depth Satellite Relay Data Loggers. *Animal Biotelemetry*, 3(21).

Rignot, E., Mouginot, J., Morlighem, M., Seroussi, H., and Scheuchl, B. (2014). Widespread, rapid grounding line retreat of Pine Island, Thwaites, Smith, and Kohler glaciers, West Antarctica, from 1992 to 2011. *Geophysical Research Letters*, 41(10):3502–3509.

Roquet, F., Charrassin, J. B., Marchand, S., Boehme, L., Fedak, M., Reverdin, G., and Guinet, C. (2011). Delayed-mode calibration of hydrographic data obtained from animal-borne satellite relay data loggers. *Journal of Atmospheric and Oceanic Technology*, 28(6):787–801.

Roquet, F., Wunsch, C., Forget, G., Heimbach, P., Guinet, C., Reverdin, G., Charrassin, J. B., Bailleul, F., Costa, D. P., Huckstadt, L. A., Goetz, K. T., Kovacs, K. M., Lydersen, C., Biuw, M., Nøst, O. A., Bornemann, H., Ploetz, J., Bester, M. N., McIntyre, T., Muelbert, M. C., Hindell, M. A., McMahon, C. R., Williams, G., Harcourt, R., Field, I. C., Chafik, L., Nicholls, K. W., Boehme, L., and Fedak, M. A. (2013). Estimates of the Southern Ocean general circulation improved by animal-borne instruments. *Geophysical Research Letters*, 40(23):6176–6180.

Roquet, F., Williams, G., Hindell, M. A., Harcourt, R., McMahon, C., Guinet, C., Charrassin, J.-B., Reverdin, G., Boehme, L., Lovell, P., and Fedak, M. (2014). A Southern Indian Ocean database of hydrographic profiles obtained with instrumented elephant seals. *Scientific data*, 1:140028.

Schodlok, M. P., Menemenlis, D., Rignot, E., and Studinger, M. (2012). Sensitivity of the ice-shelf/ocean system to the sub-ice-shelf cavity shape measured by NASA icebridge in pine island glacier, west antarctica. *Annals of Glaciology*, 53(60):156–162.

Steig, E. J., Ding, Q., Battisti, D. S., and Jenkins, A. (2012). Tropical forcing of circumpolar deep water inflow and outlet glacier thinning in the amundsen sea embayment, west antarctica. *Annals of Glaciology*, 53(60):19–28.

St-Laurent, P., Klink, J. M., and Dinniman, M. S. (2015). Impact of local winter cooling on the melt of Pine Island Glacier, Antarctica. *Journal of Geophysical Research: Oceans*, 120:6718-6732.

Thoma, M., Jenkins, A., Holland, D., and Jacobs, S. (2008). Modelling Circumpolar Deep Water intrusions on the Amundsen Sea continental shelf, Antarctica. *Geophysical Research Letters*, 35(18):L18602.

Thomas, R. H. (1979). The Dynamics of Marine Ice Sheets. *Journal of Glaciology*, 24(90):167 – 177.

Thurnherr, A. M., Jacobs, S. S., Dutrieux, P., and Giulivi, C. F. (2014). Export and circulation of ice cavity water in Pine Island Bay, West Antarctica. *Journal of Geophysical Research: Oceans*, 119(3):1754–1764.

Wåhlin, A. K., Muench, R. D., Arneborg, L., Björk, G., Ha, H. K., Lee, S. H., and Alsén, H. (2012). Some Implications of Ekman Layer Dynamics for Cross-Shelf Exchange in the Amundsen Sea. *Journal of Physical Oceanography*, 42(9):1461–1474.

Wåhlin, A. K., Kalén, O., Arneborg, L., Björk, G., Carvajal, G. K., Ha, H. K., Kim, T. W., Lee, S. H., Lee, J. H., and Stranne, C. (2013). Variability of Warm Deep Water Inflow in a Submarine Trough on the Amundsen Sea Shelf. *Journal of Physical Oceanography*, 43(10):2054–2070.

Webber, B. G. M., Heywood, K. J., Stevens, D. P., Dutrieux, P., Abrahamsen, E. P., Jenkins, A., Jacobs, S. S., Ha, H. K., Lee, S., and Kim, T. W. (2017). Mechanisms driving variability in the ocean forcing of Pine Island Glacier. *Nature Communications*, 8:14507.